Transfer dynamics of a quasiparticle in a nonlinear dimer coupled to an intersite vibration: Chaos on the Bloch sphere

D. Hennig and B. Esser
Fachbereich Physik, Institut für Theoretische Physik, Humboldt-Universität zu Berlin, O-1040 Berlin, Germany
(Received 6 April 1992)

The quasiparticle transfer in a coupled nonlinear dimer-vibration system is analyzed. The quasiparticle is subjected to both an intrasite cubic polarization nonlinearity and an intersite vibration. The system is a realization of a Hamiltonian flow on the foliated phase space represented by the Bloch sphere (density-matrix dynamics of the quasiparticle) and the plane (state of the oscillator). The analysis is performed starting from the uncoupled case for which the Hamiltonian flow on the Bloch sphere is characterized by a homoclinic structure for polarization strength above a critical value dividing the solutions into two different classes of partially trapped and untrapped transfer behavior. Then the modifications for a finite coupling, in particular, how chaos on the Bloch sphere develops, are investigated in detail, applying the Melnikov method and direct numerical integration for increasing coupling strength. The development of chaos on the Bloch sphere implies a transition from partially trapped to untrapped transfer behavior, destroying quasiparticle self-trapping.

PACS number(s): 05.45.+b, 63.20.Ls, 82.20.Rp

I. INTRODUCTION

The manifestations of nonlinearity in the transport properties of dynamic systems are numerous and result in a rich variety of the behavior of these systems controlled by parameters and initial conditions. The nonlinear discrete Schrödinger equation serves as a prototype in the investigations of these effects in recent times. The nonlinear discrete Schrödinger equation was considered, e.g., by Davydov for quasiparticle motion in biological systems [1] or in other contexts, known as the discrete self-trapping (DST) equation, for which a rich structure in the dynamic behavior was obtained [2–6]. In the DST equation the dynamics of a particle or quasiparticle are considered in the presence of a cubic-site-dependent polaronic coupling modeling energy lowering due to medium polarization, which was discussed originating with the work of Holstein [7] (see also [8,9]). Based on this discrete dynamics, Kenkre and Campbell investigated the particular case of the restriction of the transport to two sites, i.e., a dimer, and described interesting effects such as quasiparticle self-trapping for a polarization strength above a critical value [10]. Later this model was extended to include dissipation effects [11,12], and a complete analysis of the nondissipative transfer dynamics, including asymmetry effects, was presented in [13].

In this paper we address the problem of the transport properties of this nonlinear dimer model for the case of the most natural dynamic extension; namely, we include in the consideration the coupling of the quasiparticle to a longitudinal vibration along the axis connecting both molecules in the dimer explicitly. Or in the language of molecular dimers, besides the influence of the fast intramolecular polarization vibrations, which result in the polaronic energy lowering, we are interested in the effect of the slow intermolecular vibration on the transfer dynamics. This corresponds to many situations in real molecular dimers with relatively strong intramolecular interactions and weak intermolecular forces (see [14–16]).

In the present model the fast polarization effects are represented by a cubic nonlinearity, whereas the intermolecular vibration occurs roughly on the same time scale as the transfer and must be included into the consideration explicitly. The presence of chaotic dynamics and the development of a stochastic layer, which we demonstrate for our model of the coupled nonlinear dimer-vibration system, implies a transition from partially trapped to untrapped transfer behavior and has obvious applications for energy transfer occurring in molecular dimers (see, e.g., the discussion of this transition in the context of neutron scattering for the isolated dimer [17]).

In the more formal language of dynamic systems the state space of our model is characterized by a natural foliation into the direct product of the surface of the Bloch sphere and the plane representing the state of the transfer dynamics of the quasiparticle and the oscillator, respectively. We then investigate the Hamiltonian dynamics of such a coupled nonlinear system on a foliated state space, which is an interesting problem itself. For the case of an isolated dimer the flow on the Bloch sphere is characterized by the presence of a homoclinic structure, the perturbation of which may produce Smale horseshoe chaos. One important point in the analysis of the Hamiltonian dynamics of the coupled system, which we present, is then concerned with the change of the dynamics nearby the homoclinic structure, and in particular, the appearance of chaotic transfer under perturbation by the oscillator.

The model is described in Sec. II. The case of an isolated dimer using the present approach is considered in Sec. III. The coupled system is studied in Secs. IV and V using the Melnikov method as an analytical tool and numerical integration for an investigation of the influence of

different coupling strengths on the phase portrait, respectively.

II. COUPLED NONLINEAR DIMER-VIBRATION MODEL

We consider the nonlinear transfer properties of a quasiparticle between two sites in a polarizable environment (e.g., due to intramolecular polarization modes of the monomers constituting a molecular dimer), which is coupled to the longitudinal (intermolecular) vibration occurring along the axis connecting both sites. The starting point of the investigation of the coupled system is the following Hamiltonian:

$$H=H_d+H_{\rm vib}+H_{\rm int} \ . \tag{2.1}$$

Here H_d represents the Hamiltonian for the isolated nonlinear two-site system

$$H_d=\sum_{n=1}^{2}[\varepsilon c_n^* c_n-\chi(c_n^* c_n)^2]+\sum_{n,m=1}^{2}V_{nm}c_m^* c_n \ , \tag{2.2}$$

where c_n is the probability amplitude of the quasiparticle to occupy the nth site, ε is the corresponding site energy, V_{nm} is the transfer-matrix element and the cubic nonlinearity represents energy lowering due to polarization of the environment, the magnitude of which is represented by the parameter χ. The Hamiltonian (2.2) corresponds to the limit of fast polarization and slow transfer where the environment instantaneously accommodates to the quasiparticle occupation. The vibrational part $H_{\rm vib}$ describes the energy of the longitudinal vibration in harmonic approximation

$$H_{\rm vib}=\tfrac{1}{2}(p^2+\omega_0^2 q^2) \ , \tag{2.3}$$

where p and q are the momentum and the coordinate, respectively. The coupling between the dimer and the vibration is described by an interaction Hamiltonian $H_{\rm int}$, taken to be linear in the vibration coordinate q

$$H_{\rm int}=\gamma q(c_1^* c_2+c_1 c_2^*) \ , \tag{2.4}$$

where γ is the coupling constant. This off-diagonal coupling can be viewed as a modulation of the transfer-matrix element V_{nm} due to the vibration and arises from an expansion of $V_{nm}(q)$ up to first-order terms in q.

From (2.1)–(2.4) one obtains the coupled system

$$i\begin{bmatrix}\dot c_1\\ \dot c_2\end{bmatrix}=-\begin{bmatrix}\chi|c_1|^2-\varepsilon & V-\gamma q\\ V-\gamma q & \chi|c_2|^2-\varepsilon\end{bmatrix}\begin{bmatrix}c_1\\ c_2\end{bmatrix} \ , \tag{2.5a}$$

$$\ddot q+\omega_0^2 q=-\gamma(c_1^* c_2+c_1 c_2^*) \ . \tag{2.5b}$$

In (2.5) we have taken into account that the transfer-matrix elements are of an attracting type and set $V_{12}=V_{21}=-V, V>0$. Introducing the density matrix ρ with elements $\rho_{mn}=c_n^* c_m$ we pass to Bloch variables through the following definitions:

$$x_1=\rho_{12}+\rho_{21}, \quad x_2=i(\rho_{21}-\rho_{12}), \quad x_3=\rho_{22}-\rho_{11} \ . \tag{2.6}$$

It is easily seen that the variables $\bar x=(x_1,x_2,x_3)$ satisfy the identity $x_1^2+x_2^2+x_3^2=1$. The dynamics of the Schrödinger amplitudes is then described by SO(3) rotation of a vector $\bar{\mathbf{x}}=(x_1,x_2,x_3)$ lying on a surface in a vector space, the Bloch sphere. With the definitions (2.6) we can deduce the equations of motion expressed in the Bloch variables

$$\begin{aligned}\dot x_1&=\alpha x_2 x_3 \ ,\\ \dot x_2&=-\alpha x_1 x_3+(1-\beta q)x_3 \ ,\\ \dot x_3&=-(1-\beta q)x_2 \ ,\end{aligned} \tag{2.7a}$$

$$\ddot q+\omega^2 q=-\beta x_1, \quad (\bar{\mathbf{x}},p,q)\in\mathbb{S}^2\times\mathbb{R}^2 \ , \tag{2.7b}$$

where after a time scaling $t\to 2Vt$ the dimensionless parameters $\alpha=\chi/(2V)$, $\beta=\gamma/(2V)$, and $\omega=\omega_0/(2V)$ were introduced. The system (2.7) represents the coupled dynamics of the nonlinear two-site transfer problem with the oscillator, i.e., $q(t)$ influences the motion on the Bloch sphere via (2.7a), while the quasiparticle motion in turn acts as a source for q via (2.7b).

Passing to action-angle variables for the oscillator

$$p=\sqrt{2\omega I}\,\cos\Theta, \quad q=\sqrt{2I/\omega}\,\sin\Theta \ , \tag{2.8}$$

the set of Eqs. (2.7) becomes

$$\begin{aligned}\dot x_1&=\alpha x_2 x_3,\\ \dot x_2&=-\alpha x_1 x_3+(1-\beta\sqrt{2I/\omega}\,\sin\Theta)x_3 \ ,\\ \dot x_3&=-(1-\beta\sqrt{2I/\omega}\,\sin\Theta)x_2 \ ,\end{aligned} \tag{2.9a}$$

$$\dot\Theta=\omega-\beta x_1/\sqrt{2\omega I}\,\sin\Theta, \quad \dot I=-\beta x_1\sqrt{2I/\omega}\,\cos\Theta \ , \tag{2.9b}$$

and $(\bar{\mathbf{x}},I,\Theta)\in\mathbb{S}^2\times\mathbb{R}^1\times\mathbb{T}^1$.

These equations are Hamiltonian with a Lie-Poisson bracket defined on the dual space of the Lie algebra so(3)$\oplus$ so(2) with dual coordinates $\bar{\mathbf{x}}=(x_1,x_2,x_3)$ and (I,Θ). The Lie-Poisson bracket between two functions F,G: so(3)$^*\oplus$ so(2)$^*\to\mathbb{R}$ is given by

$$\{F,G\}=\sum_{i,j,k=1}^{3}c_{ij}^k x_k\frac{\partial F}{\partial x_i}\frac{\partial G}{\partial x_j}+\frac{\partial F}{\partial\Theta}\frac{\partial G}{\partial I}-\frac{\partial G}{\partial\Theta}\frac{\partial F}{\partial I} \ , \tag{2.10}$$

where c_{ij}^k are the structure constants of so(3). The structure matrix of the Lie-Poisson manifold so(3)* with elements

$$J_{ij}(\bar{\mathbf{x}})=\sum_{k=1}^{3}c_{ij}^k x_k, \quad \bar{\mathbf{x}}\in\text{so(3)}^* \tag{2.11}$$

is given by

$$\begin{bmatrix}0 & x_3 & -x_2\\ -x_3 & 0 & x_1\\ x_2 & -x_1 & 0\end{bmatrix} \tag{2.12}$$

(for a Lie-Poisson formulation of Hamiltonian mechanics, see, e.g., [18]). With respect to the Lie-Poisson bracket (2.10) the equations of motion for the Bloch vector $\bar{\mathbf{x}}$ may be written in Hamiltonian form as

$$\dot{x}_i = \sum_{j,k=1}^{3} c_{ij}^{k} x_k \left[\frac{\partial H}{\partial x_j} \right] \tag{2.13}$$

and for the vibronic part in the action-angle variables (I,Θ) the equations of motion are determined by

$$\dot{\Theta} = \frac{\partial H}{\partial I}, \quad \dot{I} = -\partial H/\partial \Theta \ . \tag{2.14}$$

The corresponding Hamiltonian function for the coupled dimer-vibration system is given by

$$\begin{aligned} H &= \alpha[x_1^2 + x_2^2 + \tfrac{1}{2}x_3^2] - x_1 + \omega I + \beta\sqrt{2I/\omega}\sin\Theta x_1 \\ &= F(\bar{\mathbf{x}}) + G(I) + H^1(x_1, I, \Theta) \ . \end{aligned} \tag{2.15}$$

In the limiting case $\beta = 0$ the unperturbed system $H^0(\bar{\mathbf{x}}, I) = F(\bar{\mathbf{x}}) + G(I)$ decouples directly into two independent integrable systems, the isolated dimer and the harmonic oscillator with integrals F and G, respectively. The transfer dynamics of the isolated nonlinear dimer as represented by the Hamiltonian F is characterized by a bifurcation in the ground state and in the flow line picture when the strength of the nonlinear coupling constant χ, or equivalently α, becomes strong enough. In particular, for $\chi > 2V$ $(\alpha > 1)$ a homoclinic structure in the flow line picture appears, the perturbation of which is one possible route to chaos. Therefore in the next section an analysis of the dynamics of the isolated dimer is given, which will be the point of departure for the consideration of the modifications introduced in the dynamics when the interaction with the oscillator in the coupled system is switched on.

III. DYNAMICS OF THE ISOLATED DIMER

We now consider the phase portrait and the solutions of the Bloch equations in the integrable case of an isolated dimer [$\beta = 0$ in (2.5)]. This will provide the basis for the application of the Melnikov method and the investigation of the modifications of the phase portrait for the coupled system in the next sections. For the decoupled transfer problem we get from (2.5) the system

$$\dot{x}_1 = \alpha x_2 x_3, \quad \dot{x}_2 = -\alpha x_1 x_3 + x_3, \quad \dot{x}_3 = -x_2 \ . \tag{3.1}$$

Expressing the Bloch variables in terms of the spherical coordinates

$$(x_1, x_2, x_3) = (\sin\theta\cos\phi, \sin\theta\sin\phi, \cos\theta) \ , \tag{3.2}$$

we can introduce the canonical conjugate variables for Hamiltonian dynamics on the Bloch sphere S^2: $\cos\theta$ and ϕ. The corresponding symplectic Poisson bracket in these variables is

$$\{F, G\} = \frac{\partial F}{\partial \phi}\frac{\partial G}{\partial \cos\theta} - \frac{\partial G}{\partial \phi}\frac{\partial F}{\partial \cos\theta} \ . \tag{3.3}$$

Representing the $\bar{\mathbf{x}}$ piece of the Hamiltonian (2.15) by the canonical variables, one finds

$$F(\phi, x_3) = \alpha[1 - \tfrac{1}{2}x_3^2] - (1 - x_3^2)^{1/2}\cos\phi \ , \tag{3.4}$$

from which applying (3.3) the equations of motion

$$\begin{aligned} \dot{\phi} &= -\alpha x_3 - x_3/(1 - x_3^2)^{1/2}\cos\phi \ , \\ \dot{x}_3 &= -(1 - x_3^2)^{1/2}\sin\phi \ , \end{aligned} \tag{3.5}$$

equivalent to (3.1), are easily derived.

An analysis of the fixed points of the system (3.5) shows that a bifurcation takes place depending on the magnitude of the nonlinearity parameter α [13]. An analogous bifurcation behavior results for polarization dynamics of a light beam propagating in a nonlinear lossless medium for which a set of equations similar to (3.1) is obtained [19]. The location and classification of the fixed points are listed below.

(i) $0 \le \alpha < 1$. There are two stable elliptic fixed points at $x_1 = \pm 1, x_2 = x_3 = 0$ (in spherical coordinates $\phi = 0, \pi, \theta = \pi/2$).

(ii) $\alpha = 1$. In this special situation there are two additional fixed points, one elliptic and one hyperbolic fixed point, which are degenerate with the elliptic fixed point at $x_1 = +1, x_2 = x_3 = 0$ $(\phi = 0, \theta = \pi/2)$ of (i).

(iii) $\alpha > 1$. There are three stable elliptic fixed points at $x_1 = -1, x_2 = x_3 = 0$ $(\phi = \pi, \theta = \pi/2)$ and $x_1 = 1/\alpha, x_2 = 0, x_3 = \pm(1 - 1/\alpha^2)^{1/2}$ $(\phi = 0, \theta = \pi/2 \pm \theta_0$, where

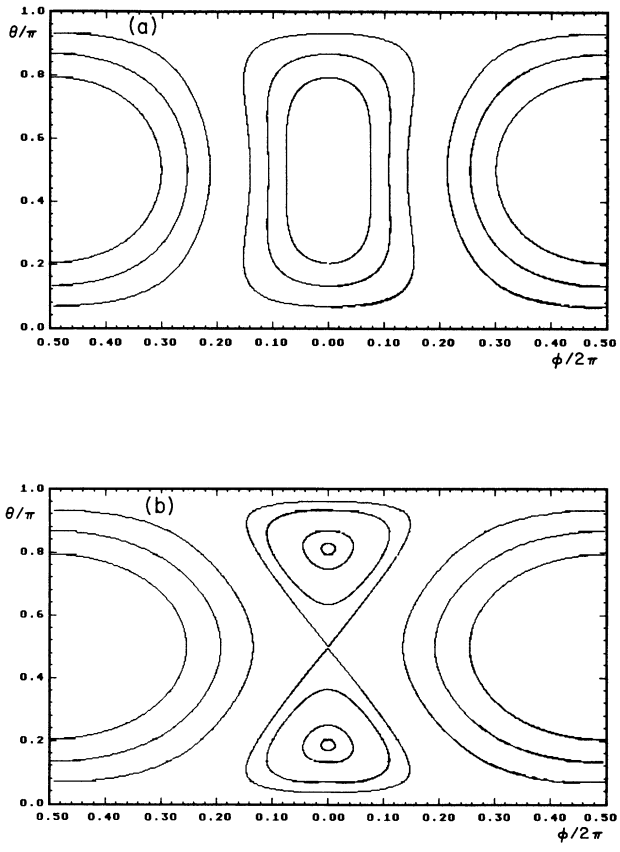

FIG. 1. Phase plots for the isolated dimer in spherical coordinates ϕ, θ. (a) Case $\alpha < 1$: Two elliptic fixed points. The dimensionless polarization strength is $\alpha = 0.9$. (b) Case $\alpha > 1$: Four fixed points. A homoclinic structure has developed, $\alpha = 1.8$. The trapped and untrapped solutions correspond to trajectories inside and outside the separatrix, respectively.

$\theta_0 = |\arccos(1/\alpha)|$. At $\phi = 0, \theta = \pi/2$ there is an unstable hyperbolic point.

The fixed points at $x_1 = +1, x_2 = x_3 = 0$ and $x_1 = -1, x_2 = x_3 = 0$ correspond to the preparation of the system as the symmetric ($c_1 = c_2 = 1/\sqrt{2}$) (ground state) and antisymmetric ($c_1 = c_2 = -1/\sqrt{2}$) (excited state) combinations of the site amplitudes, respectively. The bifurcation of the symmetric ground state into one unstable symmetric and two stable nonsymmetric states for $\alpha > 1$ as well as the stability of the antisymmetric excited state for any α is in accordance with the analysis following from the discrete self-trapping equation for the case of a dimer [2]. In the Fig. 1 we show typical phase portraits. Below bifurcation ($\alpha < 1$), the two stable elliptic centers are surrounded by elliptic-type trajectories. These orbits always cross the equator on the Bloch sphere when an oscillation is exerted and correspond to complete transfer from one site of the dimer to the other site. Above bifurcation ($\alpha > 1$), a homoclinic structure is present. Oscillations around the two elliptic fixed points embedded in the separatrix correspond to one-sided oscillations of the occupation difference $x_3(t)$, i.e., the quasiparticle is partially trapped at one side of the two-site system.

Having located and classified the equilibria, we now give the solutions outside the equilibria. From the identity $x_1^2 + x_2^2 + x_3^2 = 1$ and the conserved energy F, we deduce that

$$x_2^2 = (1/\alpha)F - \tfrac{1}{2}x_3^2 + 1/(4\alpha^2) - \alpha^2[1 - 1/(2\alpha^2) - (1/\alpha)F - \tfrac{1}{2}x_3^2]^2 . \tag{3.6}$$

Hence the solution in the Bloch variables imply the elliptic quadrature

$$\dot{x}_3 = -(\alpha/2)[(a_+^2 - x_3^2)(x_3^2 - a_-^2)]^{1/2} , \tag{3.7}$$

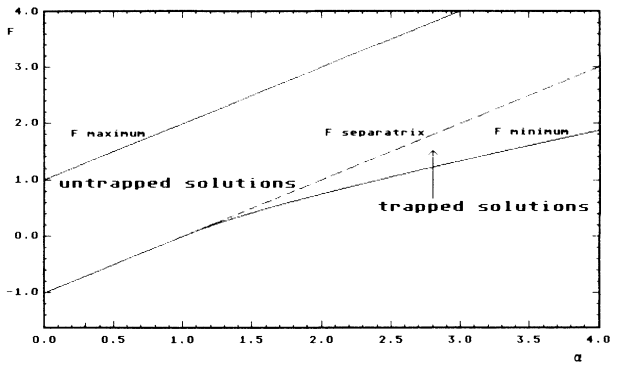

FIG. 2. Values of F in dependence on the dimensionless polarization strength. The ground-state values $F_{\min}$ are $F_{\min} = \alpha - 1$ ($\alpha < 1$) and $F_{\min} = \frac{1}{2}(\alpha - 1/\alpha)$ below and above the bifurcation point $\alpha = 1$, respectively. The value of F at the separatrix is $F = \alpha - 1$ and the maximal value of F is realized for the elliptic fixed point remaining unchanged, $F = \alpha + 1$. The regions of trapped (no change of sign in x_3) and untrapped (change of sign in x_3) transfer behavior are indicated.

where

$$a_\pm^2 = (2/\alpha^2)[\alpha^2 - 1 - \alpha F \pm (1 - \alpha^2 + 2\alpha F)^{1/2}] . \tag{3.8}$$

From the analysis of the fixed points it appears that on the Bloch sphere $\frac{1}{2}(\alpha - 1/\alpha) \le F \le \alpha + 1$ (see Fig. 2). The separatrix with energy $F = \alpha - 1$ divides the phase space (i.e., the level sets of the Hamiltonian) into two disjoint regions with different solution behavior. Correspondingly, we distinguish the following three cases depending on the corresponding energy levels $F = h^\alpha$.

Case 1: $\alpha - 1 < h^\alpha < \alpha + 1$. We obtain the following solutions in terms of Jacobian elliptic functions

$$\begin{aligned} x_1(t,k) &= \{h^\alpha/\alpha - a_+^2[1 + 2\alpha h^\alpha - \alpha^2 \operatorname{sn}^2(\tfrac{1}{2}\alpha C(t - t_0)|k) \operatorname{dn}^2(\tfrac{1}{2}\alpha C(t - t_0)|k) + \tfrac{1}{2}\operatorname{cn}^2(\tfrac{1}{2}\alpha C(t - t_\alpha)|k)]^{1/2}\}^{1/2} \\ &\quad + 1/(2\alpha) , \\ x_2(t,k) &= a_+[1 + 2\alpha h^\alpha - \alpha^2]^{1/4} \operatorname{sn}(\tfrac{1}{2}\alpha C(t - t_0)|k) \operatorname{dn}(\tfrac{1}{2}\alpha C(t - t_0)|k) , \\ x_3(t,k) &= a_+ \operatorname{cn}(\tfrac{1}{2}\alpha C(t - t_0)|k) , \end{aligned} \tag{3.9}$$

where

$$C^2 = (4/\alpha^2)(1 + 2\alpha h^\alpha - \alpha^2)^{1/2} \tag{3.10}$$

and the modulus k is given by

$$k^2 = \tfrac{1}{2}[\alpha^2 - 1 - \alpha h^\alpha + (1 - \alpha^2 + 2\alpha h^\alpha)^{1/2}]/(1 - \alpha^2 + 2\alpha h^\alpha)^{1/2} . \tag{3.11}$$

As $k \to 0$ ($h^\alpha \to \alpha \pm 1$), $(x_1(t,k), x_2(t,k), x_3(t,k)) \to (\mp 1, 0, 0)$.

Case 2: $\frac{1}{2}(\alpha - 1/\alpha) < h^\alpha < \alpha - 1$. The solutions in this energy interval correspond to periodic orbits inside the separatrix and are given by

$$\begin{aligned} x_1(t,k) &= \{h^\alpha/\alpha - (4/\alpha^2)[1 + 2\alpha h^\alpha - \alpha^2] \operatorname{sn}^2(\tfrac{1}{2}a_+\alpha(t - t_0)|1/k) \operatorname{cn}^2(\tfrac{1}{2}a_+\alpha(t - t_0)|1/k) \\ &\quad - a_+^2 \operatorname{dn}^2(\tfrac{1}{2}a_+\alpha(t - t_0)|1/k) + 1/(4\alpha^2)\}^{1/2} + 1/(2\alpha) , \\ x_2(t,k) &= \pm(2/\alpha)(1 - \alpha^2)^{1/2} + 2\alpha h^\alpha \operatorname{sn}(\tfrac{1}{2}a_+\alpha(t - t_0)|1/k) \operatorname{cn}(\tfrac{1}{2}a_+\alpha(t - t_0)|1/k) , \\ x_3(t,k) &= \pm a_+ \operatorname{dn}(\tfrac{1}{2}a_+\alpha(t - t_0)|1/k) , \end{aligned} \tag{3.12}$$

where the reciprocal modulus $1/k$ can be determined from (3.11). As $k \to 0$ [$h^\alpha \to \frac{1}{2}(\alpha - 1/\alpha)$],

$$(x_1(t,k),x_2(t,k),x_3(t,k)) \to (1/\alpha, 0, \pm(1-1/\alpha^2)^{1/2}) ,$$

and as $k \to 1 (h^\alpha \to \alpha - 1)$,

$$(x_1(t,k),x_2(t,k),x_3(t,k)) \to (1,0,0) .$$

Case 3: $h^\alpha = \alpha - 1$ (separatrix energy). For the solutions on the homoclinic orbit we obtain

$$\begin{aligned} x_1^h(t) &= 1 - 2\{\alpha + \operatorname{csch}^2[\sqrt{\alpha-1}(t-t_0)]\}/\{\alpha \coth^2[\sqrt{\alpha-1}(t-t_0)]\} , \\ x_2^h(t) &= \pm(2/\alpha)(\alpha-1)\tanh[\sqrt{\alpha-1}(t-t_0)]\operatorname{sech}[\sqrt{\alpha-1}(t-t_0)] , \\ x_3^h(t) &= \pm(2/\alpha)\sqrt{\alpha-1}\operatorname{sech}[\sqrt{\alpha-1}(t-t_0)] . \end{aligned} \tag{3.13}$$

IV. MELNIKOV FUNCTIONS

We now turn to the analysis of the system (2.9) by applying Melnikov's method [20], further developed by Holmes and Marsden in a series of papers [21–23] to show the existence of chaotic behavior in the coupled dimer-oscillator problem. In the present case we have to start from the two-degrees-of-freedom Hamiltonian system (2.15),

$$H^\varepsilon(\phi,x_3,\Theta,I) = F(\phi,x_3) + G(I) + \varepsilon H^1(\phi,x_3,\Theta,I) , \tag{4.1}$$

where the dimer part is expressed in terms of the conjugate variables $x_3 = \cos\theta$ and ϕ on the Bloch sphere according to (3.4) and we consider the case of weak coupling by introducing the dimensionless $\varepsilon \ll 1$. From the previous section we have seen that the F system has a homoclinic orbit lying on the Bloch sphere with energy

$$F(\phi^h, x_3^h) = h^0 = \alpha - 1 . \tag{4.2}$$

Let $H^\varepsilon = h > \alpha - 1$ and let $I^0 = (1/\omega)(h - h^0)$ be constants characterizing the energetic distance to the homoclinic orbit. According to the definition, the Melnikov integral is now given by

$$M(\Theta^0) = \int_{-\infty}^{+\infty} dt \{F, H^1\}[\Omega(I^0)t + \Theta^0] , \tag{4.3}$$

where $\{F,H^1\}$ denotes the Poisson bracket of $F(\phi,x_3)$ and $H^1(\phi,x_3,\Omega(I^0)t+\Theta^0,I^0)$ evaluated on the homoclinic orbit $\phi^h(t)$ and $x_3^h(t)$. If $M(\Theta^0)$ has simple zeros then the stable and unstable manifold of the homoclinic point intersect transversally, resulting in Smale horseshoe chaos [24,25]. For the Poisson bracket one gets

$$\{F,H^1\} = -\alpha\beta\sqrt{(2I)/\omega}\, x_3 (1-x_3^2)^{1/2} \sin\phi \sin\theta . \tag{4.4}$$

Evaluating the bracket on the orbit $[\phi^h(t), x_3^h(t), \Theta(t) = \omega t + \Theta^0, I(t) = I^0]$, the Melnikov function becomes

$$M(\Theta^0) = -\alpha\beta(1/\omega)\sqrt{2[h-(\alpha-1)]} \times \int_{-\infty}^{+\infty} dt\, x_3^h(t)[1-x_3^h(t)^2]^{1/2} \sin[\phi^h(t)] , \tag{4.5}$$

and with the relation $\sqrt{1-x_3^2}\,\sin\phi = \sin\theta\sin\phi \equiv x_2$ between Cartesian and spherical variables, we get with the help of (3.13),

$$M(\Theta^0) = -\alpha\beta(1/\omega)\sqrt{2[h-(\alpha-1)]}(4/\alpha^2)(\alpha-1)^{3/2} \times \int_{-\infty}^{+\infty} dt \sinh(\sqrt{\alpha-1}t)/\cosh^3(\sqrt{\alpha-1}t) \times \sin(\omega t + \Theta^0) . \tag{4.6}$$

This integral is evaluated using the method of residues, yielding

$$M(\Theta^0) = -2(\beta/\alpha)\omega\pi\sqrt{2[h-(\alpha-1)]} \times \operatorname{csch}[\omega\pi/(2\sqrt{\alpha-1}]\cos\Theta^0 . \tag{4.7}$$

As is evident from (4.7) the Melnikov function has simple zeros as a function of Θ^0, which implies that the coupled system has transversal homoclinic orbits and hence Smale horseshoe chaos in every energy level $h > \alpha - 1$ [24,25].

Now we compute the subharmonic Melnikov functions [24] for the resonant periodic orbits lying inside and outside the separatrix. The subharmonic Melnikov function can be computed in the same way with the various periodic solutions of the unperturbed problem given in Sec. III:

$$M^{m/n}(\Theta^0) = -\alpha\beta/\omega[2(h-h^\alpha)]^{1/2} \times \int_0^{mT} dt\, x_2^\alpha(t,k) x_3^\alpha(t,k) \sin(\omega t + \Theta^0) , \tag{4.8}$$

where $T = 2\pi/\omega$ is the period of the oscillator and h^α denotes the energy level of the uncoupled dimer system. If the subharmonic Melnikov function has j simple zeros in $\Theta^0 \in [0, 2\pi m/n]$, then the closed resonance curve defined by $h = h^\alpha$ breaks into a set of $2k = j/m$ periodic orbits each of period m for the Poincaré map. The period of the orbits lying inside the separatrix is given by

$$T_k = 4K(1/k)/(\alpha a_+) , \tag{4.9}$$

where $K(1/k)$ is the complete elliptic integral of the first kind. T_k is an increasing function of k with $\lim_{k\to 0} T_k = (2\pi)/(\alpha^2-1)^{1/2}$ and $\lim_{k\to 1} T_k = \infty$. The k values follow from the resonance conditions

$$4K(1/k)/(\alpha a_+) = (2\pi/\omega)m/n \tag{4.10}$$

and for each choice of m,n with $2\pi m/(n\omega)$

$>2\pi/\sqrt{\alpha^2-1}$ (4.10) can be solved to give a unique resonant orbit $[\phi^{\alpha}(t,k),x_3^{\alpha}(t,k)]$.

For oscillating motion inside the separatrix, the subharmonic Melnikov function is

$$M^{m/n}(\Theta^0)=-\alpha\beta(1/\omega)[2(h-h^{\alpha})]^{1/2}(2a_+/\alpha)\times(1-\alpha^2+2\alpha h)^{1/2}\times\int_0^{mT}dt\,\mathrm{dn}(\tfrac{1}{2}a_+\alpha t|1/k)\,\mathrm{sn}(\tfrac{1}{2}a_+\alpha t|1/k)\times\mathrm{cn}(\tfrac{1}{2}a_+\alpha t|1/k)\sin(\omega t+\Theta^0)\,, \tag{4.11}$$

where $\frac{1}{2}(\alpha-1/\alpha)<h^{\alpha}<\alpha-1$. The integral can be computed making use of the method of residues and gives nonvanishing values for $n=1$ and m even:

$$M^{m}(\Theta^0)=-4(\beta/\alpha)\omega\pi[(2(h-h^{\alpha})]^{1/2}\times\mathrm{csch}[m\pi K'(1/k)/K(1/k)]\cos\Theta^0\,, \tag{4.12}$$

with $K'(k)=K(k')$ and $k'^2=1-k^2$. As is seen from (4.12) the subharmonic Melnikov function for resonant orbits inside the separatrix has simple zeros as a function of Θ^0, hence these resonant orbits break and subharmonics of period m, with m even, should occur in the Poincaré map of the coupled system.

For periodic orbits lying outside the separatrix, the resonance condition is

$$4K(k)/(\tfrac{1}{2}\alpha C)=(2\pi/\omega)m/n \tag{4.13}$$

and the subharmonic Melnikov function is given by

$$M^{m/n}(\Theta^0)=-\alpha\beta/\omega[2(h-h^{\alpha})]^{1/2}a_+^2[1+2\alpha h-\alpha^2]^{1/4}\times\int_0^{mT}dt\,\mathrm{cn}(\tfrac{1}{2}\alpha Ct|k)\,\mathrm{sn}(\tfrac{1}{2}\alpha Ct|k)\times\mathrm{dn}(\tfrac{1}{2}\alpha Ct|k)\sin(\omega t+\Theta^0)\,. \tag{4.14}$$

We obtain for $n=1$

$$M^{m}(\Theta^0)=-2(\beta/\alpha)\omega\pi[2(h-h^{\alpha})]^{1/2}\times\mathrm{csch}[(m\pi/2)K'(k)/K(k)]\cos\Theta^0\,. \tag{4.15}$$

Since $M(\Theta^0)$ has simple zeros, a resonance closed curve lying outside the separatrix breaks into a set of periodic

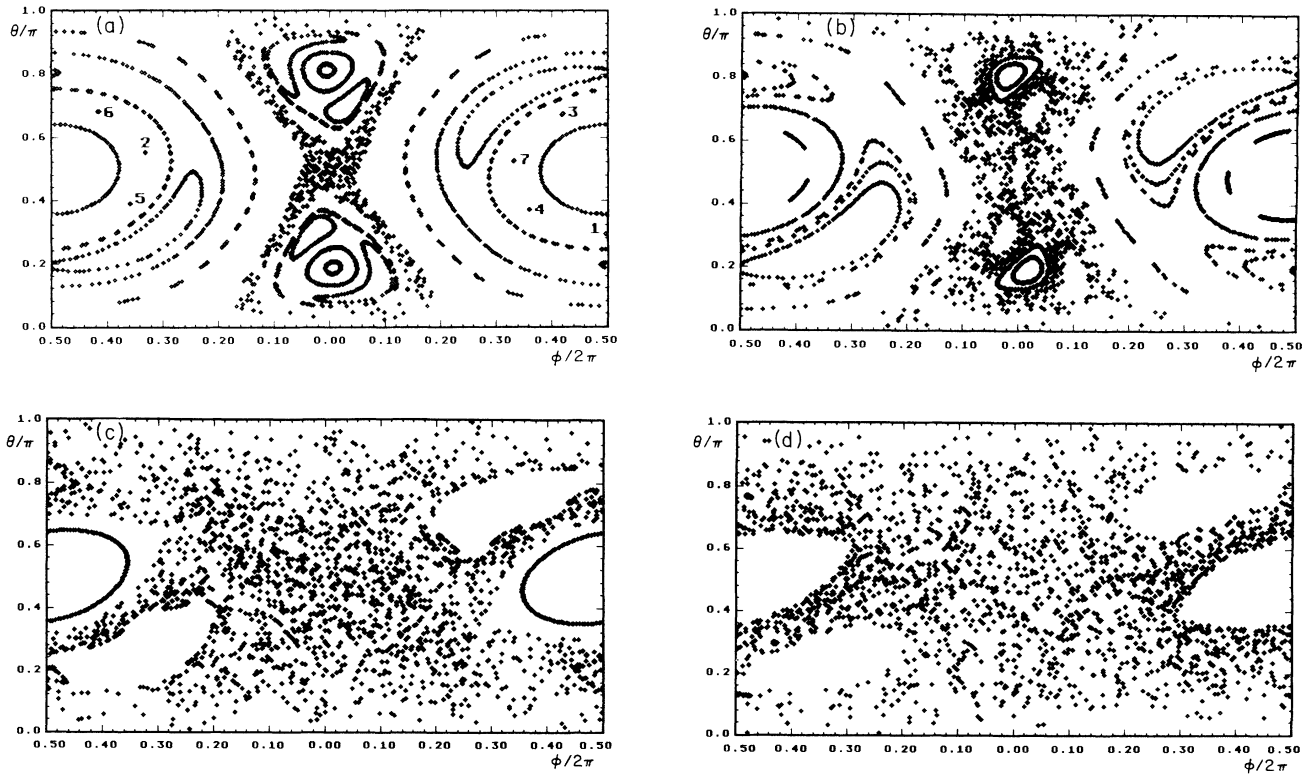

FIG. 3. Poincaré maps for the coupled nonlinear dimer-oscillator problem. The parameters are $\alpha=1.8, q_0=1.0$, $p_0=0, \omega=\sqrt{7}$. The coupling strength β increases from (a) to (d). (a) $\beta=0.06$. The stochastic layer in the separatrix region has formed. Two primary islands and a period $\frac{7}{4}$ orbit are clearly seen. Numbers indicate the order in which the periodic points appear in the surface of section. (b) $\beta=0.20$. The stochastic layer has broadened, more resonance orbits have broken off. (c) $\beta=0.50$. The structure near the elliptic points representing the ground states has completely disappeared. (d) $\beta=0.90$. The stochastic region has spread almost entirely over the Bloch sphere, leaving islands of regular motion only.

points, each of period m, in the Poincaré map of the coupled systems.

V. CHAOS ON THE BLOCH SPHERE

In the preceding section we have shown by means of the Melnikov method that the coupled dimer-oscillator system is nonintegrable and both regular and chaotic motion for different initial conditions can be expected. Therefore the phase space will be divided into regions where the system behaves chaotically and into regions of regular motion. The dynamics is determined by two facts: first, the motion near the separatrix, which will be destroyed under external perturbation; and second, a hierarchy between the perturbation frequency ω and the frequency of the unperturbed orbits $\omega(h^{\alpha})$ of the quasiparticle motion on the Bloch sphere. Whenever $n\omega = m\omega(h^{\alpha})$, with m and n relatively prime, a primary resonance occurs. Being interested in the effects of the chaotic dynamics on the transfer behavior on the dimer, we focus our attention to motion on the Bloch sphere as the corresponding part of the phase space of the coupled system by which the quasiparticle motion is represented. To this end we lower the dimension of the problem to two by taking the intersection of the energy surface $H(\phi,\theta,p,q)=h$, with the plane $q=0$, simultaneously requiring $p>0$, to give a well-defined surface of section parametrized by the variables ϕ and θ on the Bloch sphere. The set of equations (2.7) was numerically integrated for different initial conditions and each time an orbit intersects the $q=0$ plane with $p>0$, a point was placed in the surface of section. So we have a two-dimensional surface of section with the Poincaré map determining the location of successive iterates constrained to lie on the Bloch sphere. The Poincaré maps obtained by iterating 12 initial conditions are shown in Fig. 3. A periodic orbit appears in the surface of section as a finite collection of points. The Kolmogorov-Arnold-Moser (KAM) theorem [24] states that for sufficiently small perturbations of integrable Hamiltonian systems, most of the invariant closed curves are preserved. Such a quasiperiodic orbit is represented in the surface of section by a smooth curve surrounding a fixed point.

For small coupling constants β the surface of section is covered by periodic and quasiperiodic orbits. The KAM curves divide the phase space into inside and outside regions and are complete barriers to transport on the Bloch sphere, i.e., trajectories starting inside a KAM curve never reach the outer region, hence, are either confined to such a curve or are trapped between pairs of such curves. The remaining small region very close to the separatrix is covered by an irregular pattern of points belonging to chaotic trajectories. In accordance with the results of the previous section the separatrix is broken and the stable and unstable manifolds of the hyperbolic point intersect.

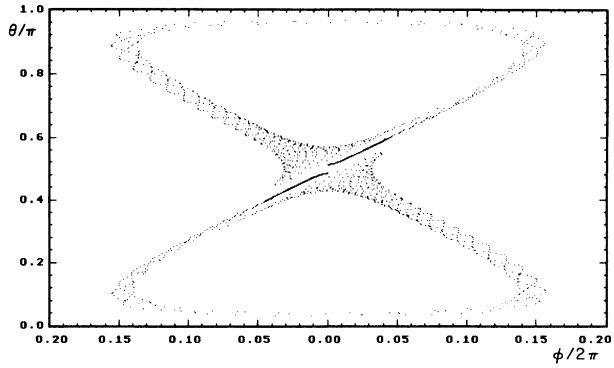

FIG. 4. Poincaré map showing the homoclinic tangle, with parameters as in Fig. 3(a).

The resulting stochastic layer connects a finite region from the inside of the separatrix with the outside of the separatrix, hence trapped trajectories that were bounded to the inner region may now escape, corresponding to partially untrapped solutions, and vice versa; untrapped solutions may become at least temporarily trapped. The width of the stochastic layer increases with the coupling strength β, as it should be expected from the discussion above. In Fig. 4 we show the homoclinic tangle obtained by iterating the Poincaré map for initial conditions lying on the stable and unstable manifolds near the hyperbolic equilibrium. Lobes created by the intersections of the stable and unstable manifolds can be identified. These lobes map one into the other at each iteration of the Poincaré map and points sufficiently near the original unperturbed homoclinic orbit may be transported by lobe dynamics, causing some loss of homoclinic trapping in the region of the Bloch sphere near the original unperturbed separatrix [26–29].

As is also evident from the analysis of the subharmonic Melnikov functions of Sec. IV resonance zones consisting of alternating hyperbolic and elliptic periodic points appear. The hyperbolic points are connected, forming heteroclinic orbits and hence when increasing β complicated stochastic dynamics similar to those for the separatrix develops. The resulting heteroclinic tangles form partial barriers to transport in phase space [26–29]. The elliptic fixed points are surrounded by regular trajectories. If we further increase β a successive breakup of KAM curves occurs and the chaotic layer becomes thicker. Finally, for relative large values of β the primary resonance zones merge, giving rise to global chaotic behavior and the whole Bloch sphere is covered with chaotic trajectories except for a few islands, i.e., except for some initial conditions in the vicinity of former elliptic points, where states remain partially trapped, most of the states are untrapped.

[1] A. S. Davydov, J. Theor. Biol. **38**, 559 (1973); Usp. Fiz. Nauk **138**, 603 (1982) [Sov. Phys.—Usp. **25**, 898 (1982)].
[2] J. C. Eilbeck, P. S. Lomdahl, and A. C. Scott, Physica D **16**, 318 (1985).
[3] J. H. Jensen, P. L. Christiansen, J. N. Elgin, J. D. Gibbon, and O. Skovgaard, Phys. Lett. A **110**, 429 (1985).
[4] S. De Filippo, M. Fusco Girard, and M. Salerno, Physica D **29**, 421 (1988).

[5] L. Cruzeiro-Hansson, H. Fedderson, R. Flesch, P. L. Christiansen, M. Salerno, and A. C. Scott, Phys. Rev. B **42**, 522 (1990).
[6] K. W. DeLong, J. Yumoto, and N. Finlayson, Physica D **54**, 36 (1991).
[7] T. D. Holstein, Ann. Phys. (N.Y.) **8**, 325 (1959).
[8] D. Emin, Phys. Today **35**, 34 (1982).
[9] D. W. Brown, K. Lindenberg, and B. J. West, Phys. Rev. A **33**, 4104 (1986).
[10] V. M. Kenkre and D. K. Campbell, Phys. Rev. B **34**, 4595 (1986).
[11] V. Szöcs, P. Banacky, and A. Zajac, Phys. Rev. A **42**, 737 (1990).
[12] G. P. Tsironis, V. M. Kenkre, and D. Finley, Phys. Rev. A **37**, 4474 (1988).
[13] B. Esser and D. Hennig, Z. Phys. B **83**, 285 (1991).
[14] D. H. Levy, J. Chem. Soc. Faraday Trans. **2**, 1107 (1986).
[15] A. Osuka, K. Marnyama, and I. Yamzaki, Chem. Phys. Lett. **165**, 392 (1990).
[16] U. Rempel, B. von Maltzan, and C. von Borczyskowski, Chem. Phys. Lett. **169**, 90 (1990).
[17] V. M. Kenkre and G. P. Tsironis, Phys. Rev. B **35**, 1473 (1986).
[18] R. Abraham and J. E. Weinstein, *Foundations of Mechanics* (Benjamin/Cummings, Reading, MA, 1978).
[19] D. David, D. D. Holm, and M. V. Tratnik, Phys. Lett. A **138**, 29 (1989).
[20] V. K. Melnikov, Trans. Moscow Math. Soc. **12**, 1 (1963).
[21] P. J. Holmes and J. E. Marsden, Arch. Rat. Mech. Anal. **76**,(2), 135 (1981).
[22] P. J. Holmes and J. E. Marsden, J. Math. Phys. **23**(4), 669 (1982).
[23] P. J. Holmes and J. E. Marsden, Commun. Math. Phys. **82**, 533 (1982).
[24] J. Guckenheimer and Ph. Holmes, *Nonlinear Oscillations, Dynamical Systems, and Bifurcation of Vector Fields* (Springer-Verlag, Berlin, 1986).
[25] S. Wiggins, *Global Bifurcations and Chaos* (Springer-Verlag, New York, 1988).
[26] R. S. MacKay, J. D. Meiss, and I. C. Percival, Physica D **13**, 55 (1984).
[27] R. S. MacKay, J. D. Meiss, and I. C. Percival, Physica D **27**, 1 (1987).
[28] V. Rom-Kedar and S. Wiggins, Arch. Rat. Mech. Anal. **109**, 239 (1990).
[29] S. Wiggins, Physica D **44**, 471 (1990).

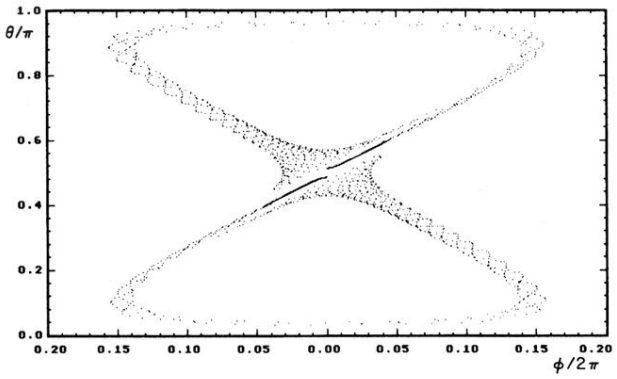

FIG. 4. Poincaré map showing the homoclinic tangle, with parameters as in Fig. 3(a).